Scientific Research Publishing

Open Journal of Marine Science, 2021, 11, 129-156
https://www.scirp.org/journal/ojms
ISSN Online: 2161-7392
ISSN Print: 2161-7384

Spatial and Temporal Variation of the Hydrological Parameters in the Wouri-Nkam Section of the Cameroon Estuary, Central African Atlantic Coast

Felix Besack[1,2,3], Ebonji Seth Rodrigue[1,2,3], Ajonina Gordon Nwutih[1,2,3], Edikin Roland Dieudonné[4], Sone Essoh Willy[1,2], Nguekeu Brice[4], Mbang Essome Junior[4], Hamadou Toume Michel-Remi[4], Onguene Raphael[5], Tomedi Eyango Minette[1,2,3]

[1]Department of Oceanography of the Institute of Fisheries and Aquatic Sciences, University of Douala, Douala, Cameroon
[2]Laboratory of Ecosystems and Aquatic Resources, Douala, Cameroon
[3]Institute of Fisheries and Aquatic Sciences of the University of Douala, Douala, Cameroon
[4]Association for the Conservation of Nature (ASCON), Douala, Cameroon
[5]Douala Institute of Technology (IUT), Douala, Cameroon
Email: besackocean@gmail.com

How to cite this paper: Besack, F., Rodrigue, E.S., Nwutih, A.G., Dieudonné, E.R., Willy, S.E., Brice, N., Junior, M.E., Michel-Remi, H.T., Raphael, O. and Minette, T.E. (2021) Spatial and Temporal Variation of the Hydrological Parameters in the Wouri-Nkam Section of the Cameroon Estuary, Central African Atlantic Coast. *Open Journal of Marine Science*, **11**, 129-156.
https://doi.org/10.4236/ojms.2021.114009

Received: July 4, 2021
Accepted: September 4, 2021
Published: September 7, 2021

Abstract

This study aimed to provide relevant knowledge about the dynamics of the hydrological parameters in the river-estuary continuum of the Wouri-Nkam river estuary for a sustainable management program. The hydrological parameters were recorded in eleven stations spanned out on the basis of population density and human activities. Water quality parameters (Temperature, salinity, dissolved oxygen, pH, Total dissolved solutes, Redox potential and conductivity) were collected in subsurface water using a multiple parameter. Surface currents and morphometric (depth and width) parameters were recorded using a drifter, sonar depth and GPS. The field measurements took placed between 18/05/2019 to 08/09/2020 and were divided into six (06) cruises. The data were later subjected to an analysis of variance (ANOVA) and Principle Component Analysis using XLSTAT 2017 (2.7 version) software. Results obtained revealed that, the water quality parameters were spatially more stable not signficant at ($df = 9$, $p < 0.05$) with a relatively low temperature (25.5˚C - 27˚C) during the wet period. The limit of the frontal zone extended to S5 (Bonalokan, 8.25 km from S1) during the snapshot of the dry period, spring phase and flood tide conditions. Inversely, during wet period, this extension reduced to S1 (Bridge) and relatively increases slightly to S3 (Bonangang) during the neap phase and ebb tides of this season. This result revealed a change in the axial gradient of about eight (08) and four (04)

kilometers during the seasonal and tidal scales (lunar and diurnal periods) respectively. These changes were also accompanied by changes in the water quality signatures, that may affect the fishery distribution and compositions. However, futures studies to buttress the results of this investigation should focus on longer time series sampling methods and model developments.

Keywords

Hydrological Parameters, Water Quality, Lunar/Diurnal Tidal Regime, Principle Component Analysis (PCA) and Wouri-Nkam River

1. Introduction

Rivers and estuarine systems around the world have attracted large numbers of people and are today affected by changes in land use, hydrological and biogeochemical cycles mainly driven by the continuous increase in population [1]. In coastal countries, especially in the developing world, cities located along the coast are exposed to intense industrialisation, rapid population growth and consequently huge human activities [2]. In a world with a progressively increase in the demand of freshwater for human consumption, agricultural and freshwater fisheries, the previous activities are oppositely affecting the quality and quantity of water resources in fresh and estuarine systems. Furthermore, climate changes that have caused increase in temperature and salinity of estuarine waters with a direct influence on the behaviour and distribution of zooplankton communities are becoming more intense [3]. Some studies have shown that, human induced changes in salinity affect aquatic ecosystems and the marine species that dwell within them [4]. In this sense [5] have highlight that, joint changes in salinity and temperature yield a stronger indicator of human impact on climate change than either salinity or temperature alone. These numerous revelations have continuously increased the need for understanding the functioning of estuaries and their relation with the coastal environment.

According to [6], the factors affecting the vibrating regime of tropical estuaries are; 1) grouped under, 2) riverine (water discharges and levels in the river, river water chemical and physical properties, thermal regime, sediment runoff, etc.), 3) marine (water level, currents, tides, wind waves, seawater physical and chemical properties, alongshore sediment flux, etc), 4) geological and physico-geographic (climate, relief, soil-vegetation cover, etc.) and 5) anthropogenic (runoff regulation, waste discharge, dredging and channel improvement operations, navigable channel construction, etc.). These factors are different for different estuaries and may vary over time for the same estuary [6]. For example, in San Francisco Bay, phytoplankton biomass, community composition and productivity responses according to variability in river flow differ between the river-dominated northern reach and the South Bay, a lagoon-type estuary [7]. In upper estuaries, where freshwater from the riverine end and brackish water from

estuarine end joint and mixt (tidal intrusion frontier), the water masses are generally characterized by small scales eddies due to mixing, stratification, frontogenesis (generation or intensification of a frontal zone) and frontolysis (collapse or dissipation of frontal zone) activities. The tidal influence on these zones seems to appear when denser water intrudes into a basin of buoyant water and plunges downward as a negatively buoyant gravity current [8]. These regions are important not only due to their contribution to the transport of heat, momentum, buoyancy and tracer but also their crucial role in the formation and distribution of biological component of aquatic environments [9] [10]. [11] discussed the important role of these frontal zones in the composition, abundance and distribution of many algal species as well as the primary productivity of estuaries. Furthermore, [12] [13] used these zones to understand and described the processes controlling the distribution of aquatic fauna in small scale systems. These authors also concluded that, the saline intrusion front can serve as barriers in the transferring of nutrients and pollutants from rivers to estuaries and vice versa.

Despite the ecological, biological and chemical importance of salt fronts, their dynamics over time scale ranging from hourly/daily (fresh water pulses and local wind) to weeks (spring-neap tides conditions) and finally months (seasonal river discharge and change in wind regime) remains unwell investigated in tropical estuaries of the developing world. The few existing studies on the salt intrusion dynamics in these estuaries are generally based on mathematical models [14] [15] [16]. However, these models require a well structure dataset from intense and well organised field measurements for their calibration, verification and validation. The availability of such a data set may not be an easy task since they are time and energy consuming and also demand an important funding.

Like in the other tropical estuaries, the Cameroon estuary is characterized by few studies related to this topic, which are limited in its lower and middle section. They concern the water quality evolution [2], hydrological regime [17], water level dynamic [18], implication of tides on the hydrological dynamics [19], dynamics of the turbidity maximum near the upstream limit of the salinity intrusion zone [20], levels, patterns and ecotoxicology of persistent organic pollutants in sediments [21]. All the above investigations have been carried in the lower estuary, leaving the upper section unknown despite its direct contact with the local population (high human impact) of the city of Douala to whom it provides the necessary ecosystems services (aquatic animals as food, medical plants, sand for construction, fresh water for human consumption etc).

This paper focus on the understanding of the hydrological parameters (water quality parameters, surface current and discharges volumes) dynamics in the Wouri-Nkam channel of the Cameroon estuary *i.e.*, between the Oligohaline (Bridge) and the Limnic ends (Bona'Anja) from daily to seasonal time scales passing through the lunar cycle. This is a contribution to the monitoring and future development of a sustainable management initiatives and tools geared towards enhancing future fisheries productivity through protection of nursery

grounds as well as endangered species and understanding of impacts of climate change on future projects.

2. Material and Methods

2.1. Study Site Description and Location of Sampling Stations

The Cameroon estuary is located between latitude 04˚01' and 04˚06'North and longitudes 09˚40' and 04˚40' 09˚45' East (Figure 1). The Wouri Estuary (Figure 1) is one of the largest in the Cameroon estuarine system in terms of surface area (625 km^2) and mean annual discharges (340 m^3/s) [17]. It has attracted more than 3 millions inhabitants in its vicinity (upper section of Wouri-Nkam) making the city of Douala the most populated and consequently the economic capital of the Republic of Cameroon. This city bears about 75% of the industrial fraction and produce more than 30% of the national income of the country [22]. The major attractive activities include industrial development accompanied by intense urbanization, agriculture, sand mining, fishing, ecotourism and navigation. This area also bears a diversity of habitats to numerous fish species for feeding, reproduction and nursery activities. It is an important migratory corridor for diadromous species (polydactylus sp., skate fish, manatee, pseudotolithus sp. etc.) that are pillars of the local fishing ground and furthermore the local economy. Some of the important neighbourhoods whose activities are directly connected to this study area are Bonaberi-Deido (Pont Wouri), Akwa nord, Bonamouang, Bangué, Bonalokan, Yassem, Bossamba, Bonepea etc. (Figure 1). Their different characteristics are presented in Table 1. The watersheds that influence

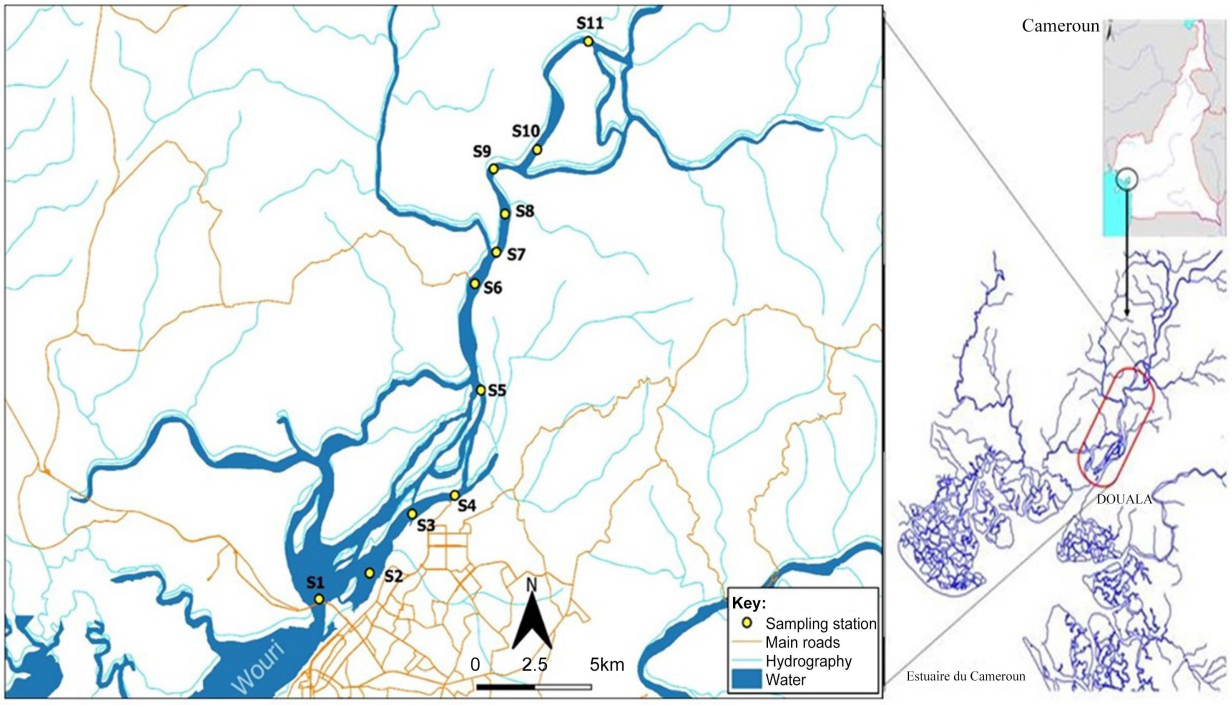

Figure 1. Location of the Wouri-Nkam section of the Cameroon Estuary the various sampling stations and the corresponding neighbourhoods of the city of Douala (D).

Table 1. Chronogram of field measurements (surveys).

N°	Period	Tidal phase	Season (hydrological period)
1	11-13 May 2019	Neap tide (38 - 41)	Average season/transition season (average waater)
2	18-20 May 2109	Spring tide (90 - 102)	
3	05-06 Jul. 2020	Neap tide	
4	14-15 Nov. 2020	Spring tide (105 - 109)	Dry season (Low water periods)
4	04-05 Jan. 2020	Neap tide (105 - 109)	
5	13-15 Jan. 2020	Spring tide (75 - 90)	
6	17-18 Sep. 2020	Spring tide (110 - 113)	Wet season (High water periods)
7	09-10 Oct. 2020	Neap tide (34 - 38)	

the hydrology of this portion of the estuary are; the Besseke (in the lower part), the Mbanya, Tongo bassa, Mboppi, Ngongué (in its middle section), river Nkam and Makombe (drain in the upper section) (**Figure 1**). The equatorial climatic regime of this zone is bimodal with a dry (hot) season of about 6months (October-March) and a rainy (wet) season that also lasts from April to September. During the dry season, the Harmattan wind blows from the Sahara in the north, causing low humidity and high atmospheric temperatures; while in the rainy season, the moisture laden winds that blows from the Gulf of Guinea in the south bringing high humidity and rain that sometimes generates floods. The average river discharge is 340 m^3/s, value laying between 65 m^3/s in February (minimum) and 600 m^3/s in September (maximum) [17]. This estuary is also characterized by a low-lying relief (with mangroves vegetation) with altitude varying from 03 to 100 meters above the see level [23]. The tidal regime is semi-diurnal with tidal ranges changing from mesotidal (values > 2 m) to microtidal (values < 2 m) [18] [24]. The maximum depth (after dredging) of the entire estuary is 25 meters *i.e.*, along the harbour channel. This depth reduces to 6 meters around the Bonaberi Bridge (S1). During one tidal cycle, the tidal wave can propagate more than 60 km upstream from the mouth [17]. Also, this estuary is described as hypersynchronous [25] *i.e.*, the tidal amplitude increases progressively towards the upper estuary, reaching its maximum value at 30 km away from the mouth before decaying in the fluvial narrow sections [18].

2.2. Field Preparation and Data Collection

The field measurements were spanned out from May, 2019 to October, 2020, precisely during flood and ebb tidal conditions of the high, average and lower water regimes (hydrological periods) with respect to the spring/neap regime (**Table 1**). The values of the tidal coefficients together with the flood/ebb conditions were taken from the tide for fishing chart of the littoral region of the Cameroon coast (https://tides4fishing.com).

Before the local cruises, the map of the Cameroon estuary was used to select the different sampling stations. The distribution of these stations took into ac-

count the spatial heterogeneities due to natural or anthropogenic effluents and population activities coupled to banks occupation (Figure 1, Table 2). All the eleven (11) sampling stations were selected for the monitoring of the water quality parameters (Temperature, salinity, dissolved oxygen (DO), pH, Total dissolved solutes (TDS), Oxydo-reduction potential (ORP) and conductivity), surface currents and morphometric (depth and width) parameters. The surface current and morphometric parameters were further used for the computation of the river discharge volume (Equation (2)).

The displacement from one point (station) to other within the estuary was done using a flying-boat (40 horse feet) and each point was geo-localized using a GPS of brand GARMIN (version, GPS map 64). In each sampling station (S), the water quality parameters were measured using a multiple parameter probe of brand HANA HI 2837. Six (06) sampling were made covering the surface and bottom of the left and right banks including the middle portion. The mean value obtained during this exercise was registered as the sample variable for that sampling section.

Surface currents and morphometric parameters were measured using a set of instruments composed of a drifter, a measuring tape and/or a GPS and a monobeam sonar depth.

For surface current, the drifter was deployed in water and allowed to derive for a distance of 20 meters. The time of this displacement was recorded using a stopwatch and the surface current was computed through Equation (1). Three (03) elementary measurements representing the middle and the various river banks (left and right) were conducted in each transect or sampling station (100 meters long). During this activity, the distances separating the various banks were given by the GPS and/or the measuring tape. This distance (width), together

Table 2. Presentation of the selected sampling stations.

Point Names	Latitudes	Longitudes	Distance from S1 and Descriptive characteristics
Pont Wouri (S1)	4.073108	9.696038	Closest to the middle estuary, intense human settlement and industrialization (Presence of Cements industries and the Douala harbour).
Akwa Nord (S2)	4.077512	9.714731	0.8 km/High settlement, fishing land and intense dredging activities.
Bonagang (S3)	4.085502	9.719025	3.51 km/Moderated urbanization, sand dredging and strong land reclamations activities.
Bangue (S4)	4.110945	9.74996833	3.79 km/Housing, sands extraction/dredging
Bonalokan (S5)	4.14722167	9.75700333	8.23 km/Sediments extraction and fishing ground
Yassem (S6)	4.18522167	9.75408833	12.31 km/Fishing and agricultural village (low urbanization)
Bonagando (S7)	4.19314333	9.763125	15.51 km/Fishing village poor housing
Ngombe (S8)	4.20818833	9.76855833	16.84 km/Fishing village poor housing
Bossamba (S9)	4.22473667	9.76159833	19.61 km/Agricultural and Fishing village with low settlement
Bonapea (S10)	4.2313433	9.77869167	23.62 km/Fishing village
Bona'Anja (S11)	4.26832667	9.80019333	28.36 km/Sand dredging, Agricultural, fishing/aquaculture (Aquaculture centre) and Tourism development with moderated urbanization.

with the depth obtained from the acoustic sonar depth were used for the computation of the cross-sectional areas.

$$V = \frac{D}{T} \tag{1}$$

where V, D and T represent the velocity, distance travel and time taken.

This velocity, together with the cross sectional area were used in the understanding of mass transport (discharge volume) per unit width of a segment computed using Equation (2).

$$Q = V \times \Omega \tag{2}$$

with Q being the discharge volume per unit area, V is the surface current and Ω the water cross sectional area computed from the water depth and width of the various sampling sections. All the above water quality and hydrometric parameters were collected during flood and ebb tides conditions of the same semi-diurnal cycle with respect to neap/spring phase of the moon at the different hydrological periods (seasons) (Table 1).

2.3. Statistical Data Analysis

The data obtained following the above methodology were reorganized and grouped according to inter annual, seasonal, lunar and daily scale. They were further subjected to analysis of variance (ANOVA) and multivariate statistical procedures. ANOVA was performed on the different temporal (inter-annual, seasonal, lunar and diurnal) and spatial (stations) scales to verify the homogeneity between the various parameters. The principle component analysis (PCA) was conducted not only to established linkages between water quality parameters among themselves, water quality parameters and hydrodynamic forces but also to regroup the different sampling stations according to their affinities and dissimilarities. This method has been widely used to analyses physical and chemical parameters in similar aquatic environments [26] [27]. These statistical analyses were performed using the 2017 version of XLSTAT software.

3. Results

3.1. Spatial and Temporal Evolution of Water Quality Parameters

We firstly investigated the spatial and temporal evolution of the water quality parameters in this channel during different hydrological periods (wet, dry and intermediate season), Lunar and tidal phases, as well as inter annual regarding the average water only.

Intra-seasonal dynamics of the monitored water quality parameters

This scale comparison was performed to understand the dynamics of water quality parameters during the different seasons of the year. The results of this observation are presented in Figure 2 below.

Tidal variability of monitored water quality parameters

Secondly, we examined the spatial evolution of the water quality parameters in

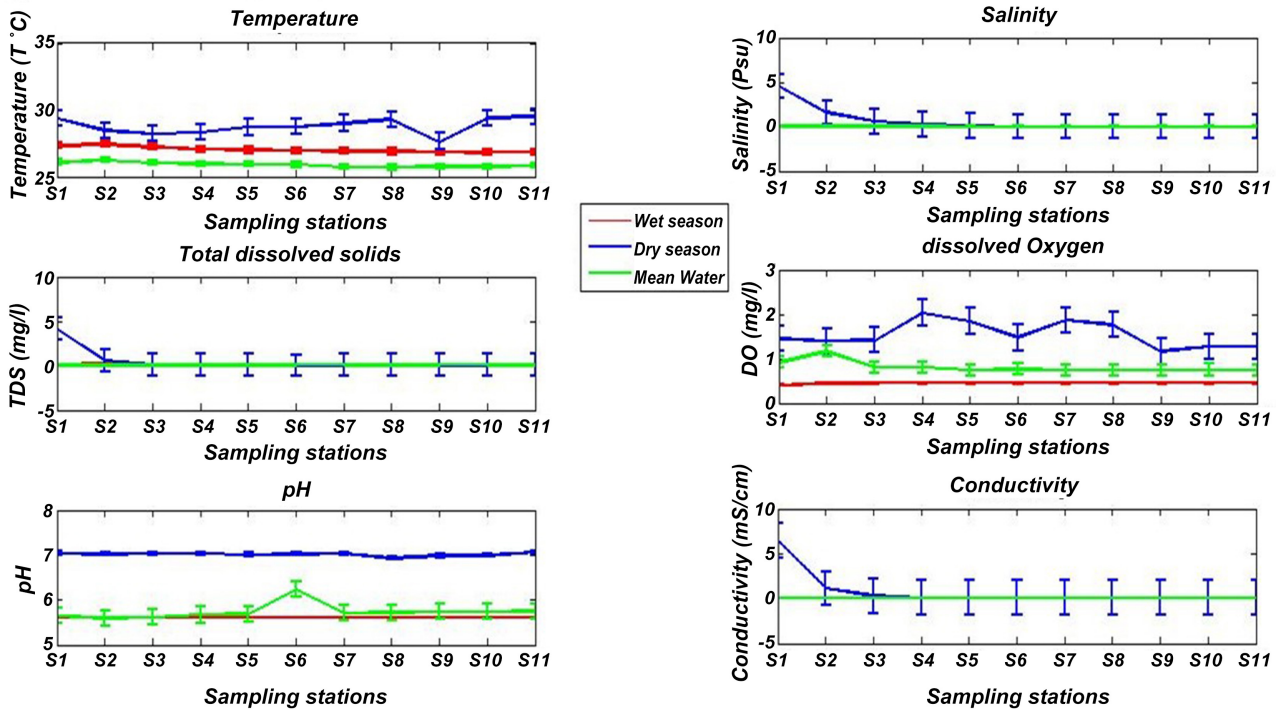

Figure 2. Dynamics of seasonal and spatial snapshot of water quality parameters.

the channel at different lunar phases (Figure 3). The diel variation was monitored under flood and ebb tides conditions (Figure 4).

- Inter-tidal variation (lunar influence)
- Diurnal (Diel) variation of monitored water quality parameters

***Inter-tidal comparison between* 2019 *and* 2020**

The Inter annual comparison between the year 2019 and 2020 was performed by comparing the data of the May 2019 with those of July and November 2020 since they were all collected during the same hydrological season. This season was chosen not only because it has the largest dataset but also better represent the average yearly conditions. The result obtained are shown in Figure 5 below.

Tempertaure: the highest temperatures (28.78˚C ± 0.59˚C) were recorded during the dry period (blue line) while the lowest temperature values (25.89˚C ± 0.17˚C) were noted during the mean water period (green line) rather than the expected wet period (red line, 27.00˚C ± 0.21˚C) (Figure 2). Similarly, the most dynamic (greatest standard deviation or longest errorbars) was the dry period, followed by the wet and finally the mean water period. Looking at the lunar scale (tidal regime), spring tide was relatively warmer (28.39˚C ± 1.04˚C) than it neap (26.04 ± 0.15) tide snapshot (Figure 3). Also, this period showed an axial gradient with warmer upstream (S5 to S11). This spatial evolution was eroded during the neap (blue line) tide phase. Regarding the diurnal scale (Figure 4), the ebb tide condition with its mean temperature value of 29.89˚C ± 1.16˚C was slightly warmer compared to its corresponding flood phase (28.39˚C ± 1.04˚C). The inter tidal comparison between the year 2019 and 2020 (Figure 5) revealed

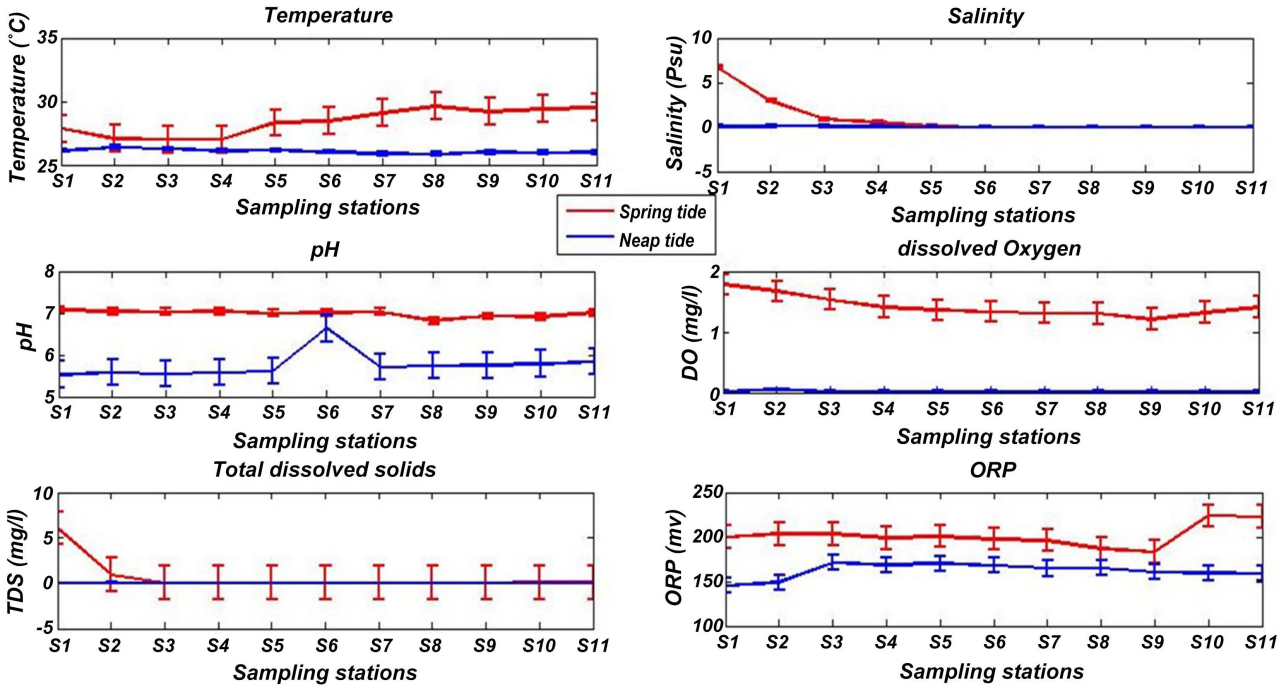

Figure 3. Lunar evolution of water quality parameter (spring tide with tidal coefficient greater than 90 and neap conditions with coefficient lesser than 40).

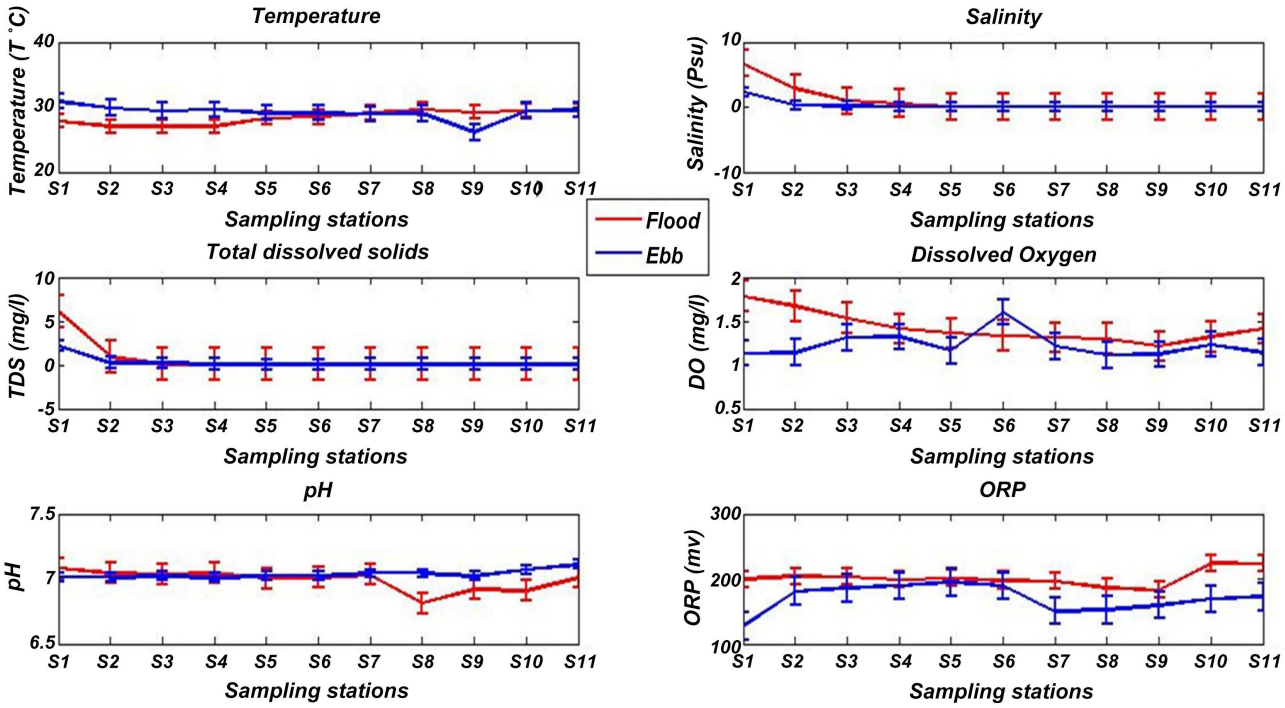

Figure 4. Diurnal evolution of monitored water quality parameters during during the dry condition.

that, the year 2019 was found to be warmer (30.74˚C ± 0.85˚C) compare to the year 2020 (28.39˚C ± 1.04˚C). However, the spring of the 2020 was more dynamic than its corresponding 2019 spring tide condition. Furthermore, the temperature

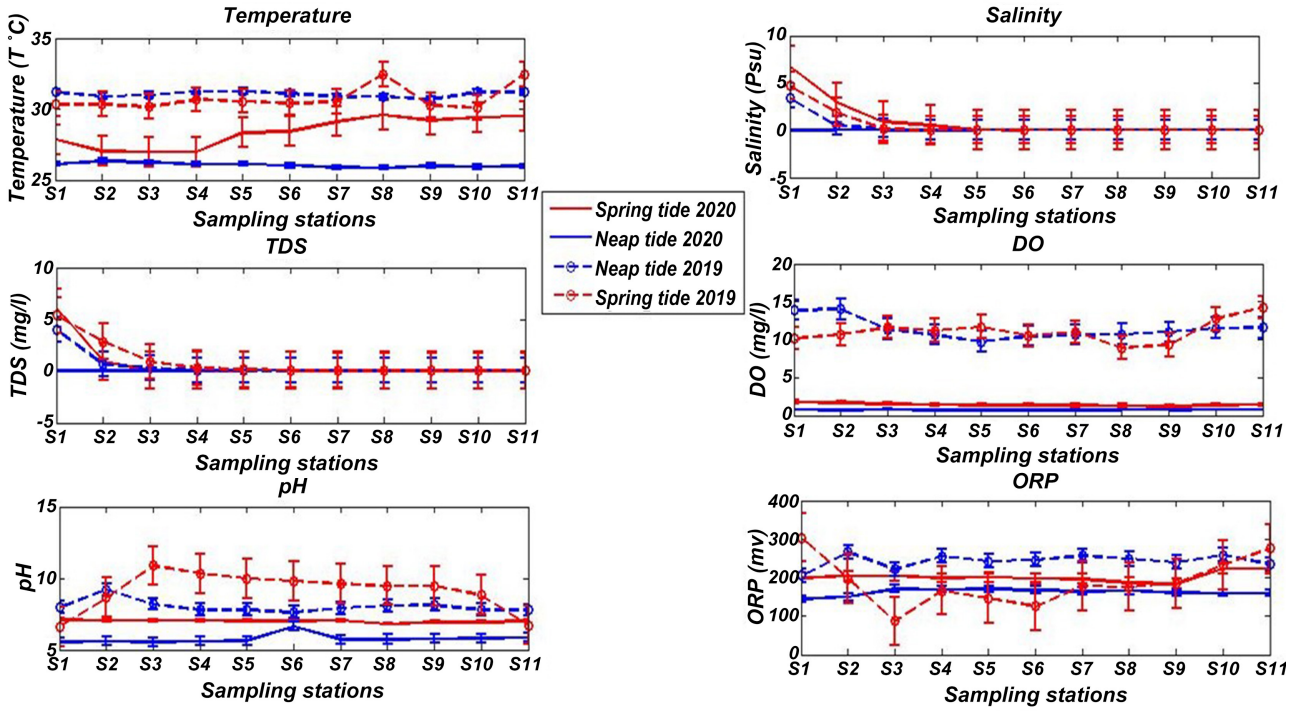

Figure 5. Camparing tidal conitions of similar intensities between 2019 and 2020.

gradient that was eroded in 2019 (broken red line) reappears during the spring tide regim of the year 2020 (red line).

Salinity: at seasonal scale (Figure 2), this section of the estuary was completely dominated by freshwater (0.0073 ± 0.017 psu) during the average (green line) and wet season (0.0036 ± 0.0067 psu) (red line) respectively. Oppositely, the residual dry period snapshot highlighted an axial gradient dividing this zone into two sections; the oligohaline site made up of S1, S2 and S3 with salinity values of 4.5, 1.57 and 0.55 psu respectively and a limnic zone ranging from S4 to S11 having null (0.00 psu) salinity values. This division is also noticeable at lunar scale; during spring tide (red line) (Figure 3). However, the oligohaline zone extended to S4 during this period. The diurnal scale presented salinity gradients during both flood and ebb phases (Figure 4), with a more penetrating gradient during the flood tide condition (red line). The inter comparison of salinity distribution between 2019 and 2020 (Figure 5), revealed that, the spring tide of 2020 was more intense and extended the salinity trace at S4 (s = 0.5 psu) while it corresponding spring condition in 2019 was limited to S3 (s = 0.1 psu). Oppositely the neap tide regime of 2019 (S1 = 3.4 psu) was more intense compare to that of 2020 (S1 = 0.1 psu). The length of the errorbars in Figures 2-4 showed that, the dry period, spring phase and flood tide are the most dynamic (longest errorbars) with respect to their seasonal, lunar and diurnal scales. The spatial and temporal trends observed for salinity is similar to that presented by Conductivity since they are both conservative properties of sea water. For this reason the latter variable/parameter will not presented again.

Total Dissolved Solids (TDS): TDS showed relatively higher values (0.47 ± 1.22 g/l) during the dry period (blue line) compared to the mean (green line) and wet season (red line) whose mean TDS values are 0.806 ± 0.0053 g/l and 0.035 ± 0.0067 g/l respectively. Concerning the lunar evolution (Figure 3), the spring phase of tide (red line) presented a greater TDS mean value (0.667 ± 1.81 g/l) with an axial gradient (lower to that observed in salinity) while the neap tide period (blue line) presented a lower (0.020 ± 0.0088 g/l) and nearly constant spatial distribution. This spring gradient gives the highest values at S1, followed by a decrease in the upstream. At diurnal scale (Figure 4), flood tide condition presented greater TDS values (0.666 ± 1.81 g/l) compared to it corresponding mean ebb TDS values of 0.27 ± 0.63 g/l. Looking at its inter annual evolution (Figure 5), TDS showed a wide variability. Indeed, the spring phase of the year 2019 has greater TDS values (0.89 ± 1.70 g/l) compared to its equivalent spring phase of 2020 (0.667 ± 1.81 g/l). Paradoxaly, the neap phase of 2020 had an unexpected greater TDS values. The overall spatial distribution of this parameter with its axial gradient revealed its consrvative character of brackish water in this estuary.

Dissolved oxygen (DO): the seasonal variability of DO (Figure 2) exposed a more dynamic dry period (blue line) with the greatest value (1.54 ± 0.28 mg/l) compare to the average water value of 0.806 ± 0.12 mg/l (green line) and the wet period value 0.44 ± 0.215 mg/l (red line). Figure 3 and Figure 4 of both lunar and diurnal tide conditions showed that, the spring phase with a mean DO value of 1.4 ± 0.1 mg/l and flood tide with mean DO of 1.42 ± 0.17mg/l presented the better oxygenation periods compared to their respective neap and ebb phases. The interannual evolution (Figure 5) showed that, the year 2019 was far better oxygenated (11.08 ± 1.5 mg/l) than the year 2020 (1.4 ± 0.1 mg/l). The spatial trend in DO reveal a peaks values at S1 in the spring and flood tide (Figure 3 and Figure 4). This trend was the case at inter-annual scale.

Oxidation-Reduction Potential/Redox potential (ORP): the spring tide (red line) has greater values than their corresponding neap tide (blue line). Also the lunar evolution (Figure 4) revealed that, during spring tide, S10 and S11 presented the highest values (greater than 220 millivolts). The diel comparion showed that, the flood tide with values ranging from +200 to 230 mV dominated the ebb tide whose values lied between +100 mV (S1) to +200 mV (S5). The spatial trend also presented dominating S10 and 11 in flood. Here S1 and S2 have the lowest values of ORP. When comparing the inter annual lunar and diurnal phase (Figure 3), the neap tide of the year 2019 presented greatest values (+200 to +250 mV), followed by the spring phase of the year 2020 (+200 to 230 mV). The spring tide of 2019 was very dynamic with values ranging from +100 to +300 mV, with the lowest point (+100 mV) in S3 and a highest transect at S1 (+300 mV). The greater ORP values (positives) were recorded during the neap phase of 2020 (blue line) (Figure 5).

Hydrogen potential (pH): at seasonal scale (Figure 2), the pH value was nearly neutral (a nearly constant pH vaue of 7) during the dry period (blue line).

The mean water and wet periods showed pH values lower than 6. The pH value during spring tide was close to neutral without fluctuations while that of the neap phase showed acidic properties with pH around 5.5, except in S6 where a nearly less acidic value of 6.6 was recoded (Figure 3). The diurnal snapshot (Figure 4) showed a slightly neutral pH during both flood and ebb tides. Despite the poor distinction within the diurnal scales, the flood tidal condition presented a acidic character in its upstream section (from S8 to S11).

Surface current and dischaarge volumes variation (Hydrometric parameters): the seasonal variation (Figure 6) showed that, the wet season has the greatest surface currents (red line), followed by the mean water (green line). Also, all the curves presented a typical axial gradient with an increase in surface current going upstream. The surface currents do not changes its flowing direction during the wet, dry and the average water conditions (Figure 6). On the other hand, the lunar and the diurnal scale presented a bidirectional flow with upward and downward flows represeented by negative and positive signes respectively (Figure 6). However, the bidirectional flow obtaind at diurnal snapshot is slighly stronger and more extended compared to that of the lunar conditions. These results highlighted that, in the diel or diurnal conditions snapshot, the ssurface current reverse reached up to S7 (Bonagando, 15.5 km from S1) meanwhile, at a lunar scale, this bidirection flow erodes dowward at S6 (Yassem, 12 km from S1). The discharge intensities also presented the same trends as surface current at seasonal scale *i.e.*, wet > averagewater > dry period. However, the discharge curve presented a gradient showing high values in S1 (Figure 6).

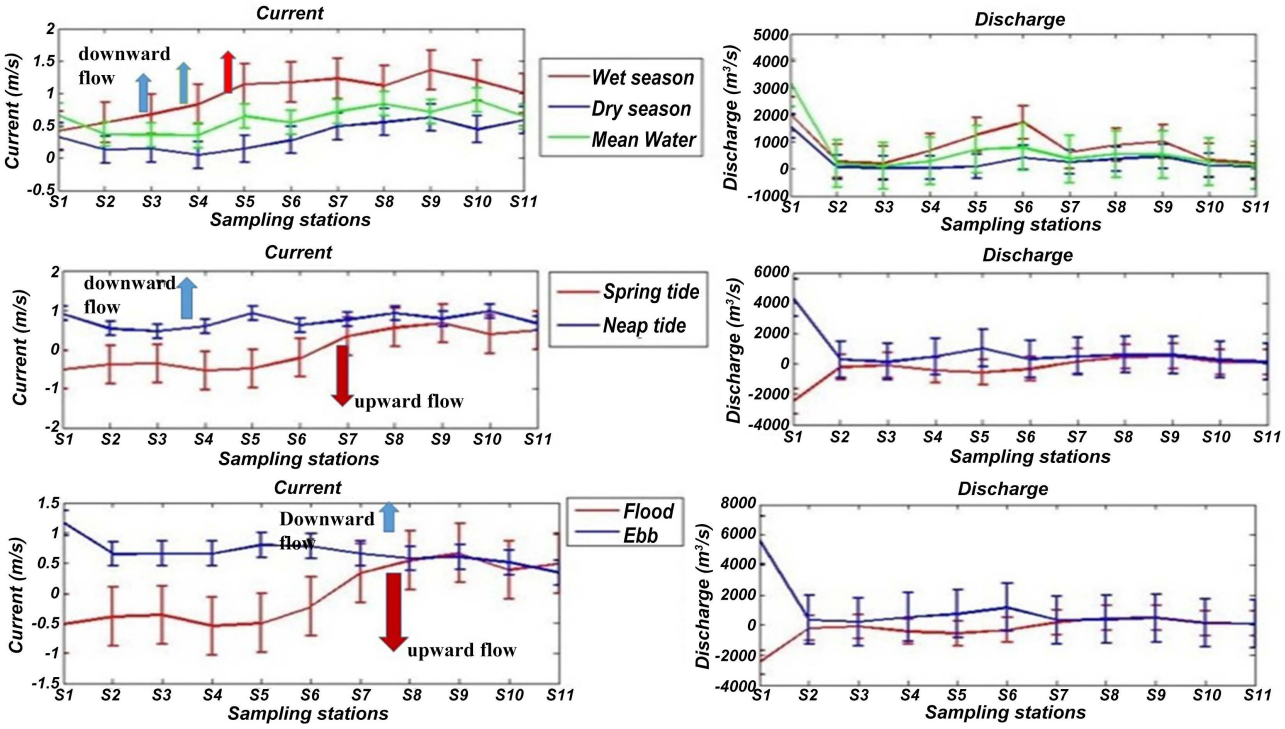

Figure 6. Spatial and temporal dynmaics of surface currents showing landward (negative) and seaward (positive) direction.

The discharge volumes passing through a section also presented a gradient with high walues at S1 during both lunar and diurnal scales. These trends revealed that, the lowest dischages volumes were upstream (towards S11). The length of the errobars also revealed that, the wet season was the most dynamic at seasonal scale. The spring phase and flood tide showed more spatial dynamic conditions compared to their corresponding neap and ebb tides. The trend was not true for discharge volumes in which the more spatial dynamics were, ebb tide, neap phase and the mean water for the diurnal, lunar and seasonal scales (Figure 6).

3.2. Interactions between Hydrological Parameters

The bi-plots of the dynamics of hydrological parameters (temperature, salinity, pH, TDS, DO, ORP, surface current and freshwater discharge) in the estuary-river interface of the Cameroon estuary are presented in the Figures 7-10 below. The results obtained from this analysis are presented at different time scales in order to reveal how this milieu changes with time. The factorial plans (F1 and F2) obtained from the biplots showed that more than 60% of the variables were expressed, with the F1 plan having a greater variance compared to F2.

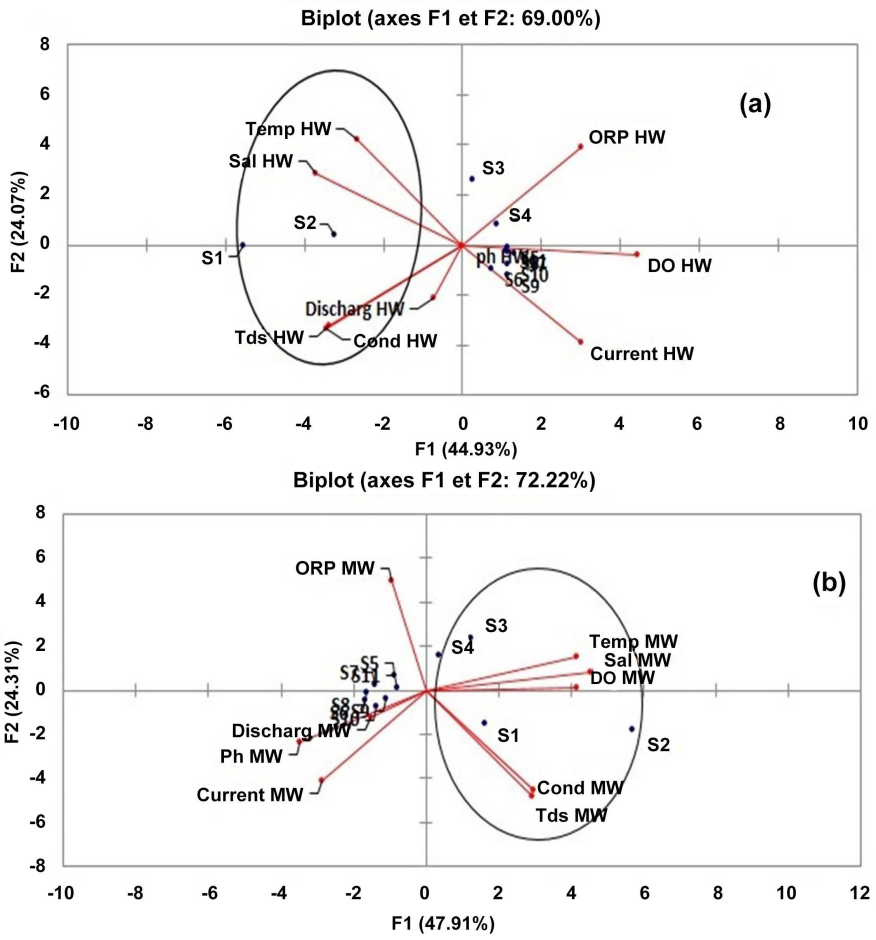

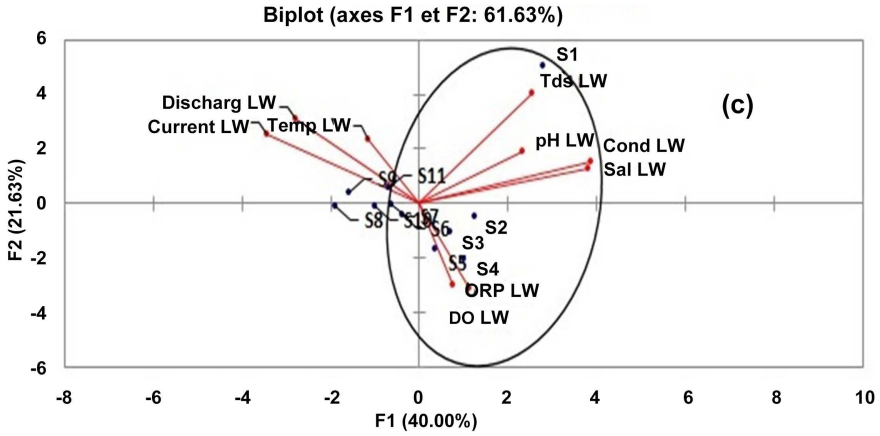

Figure 7. Seasonal change in hydrological parameters showing their different links during high water (a), mean/Average water (b) and Low water regimes (c).

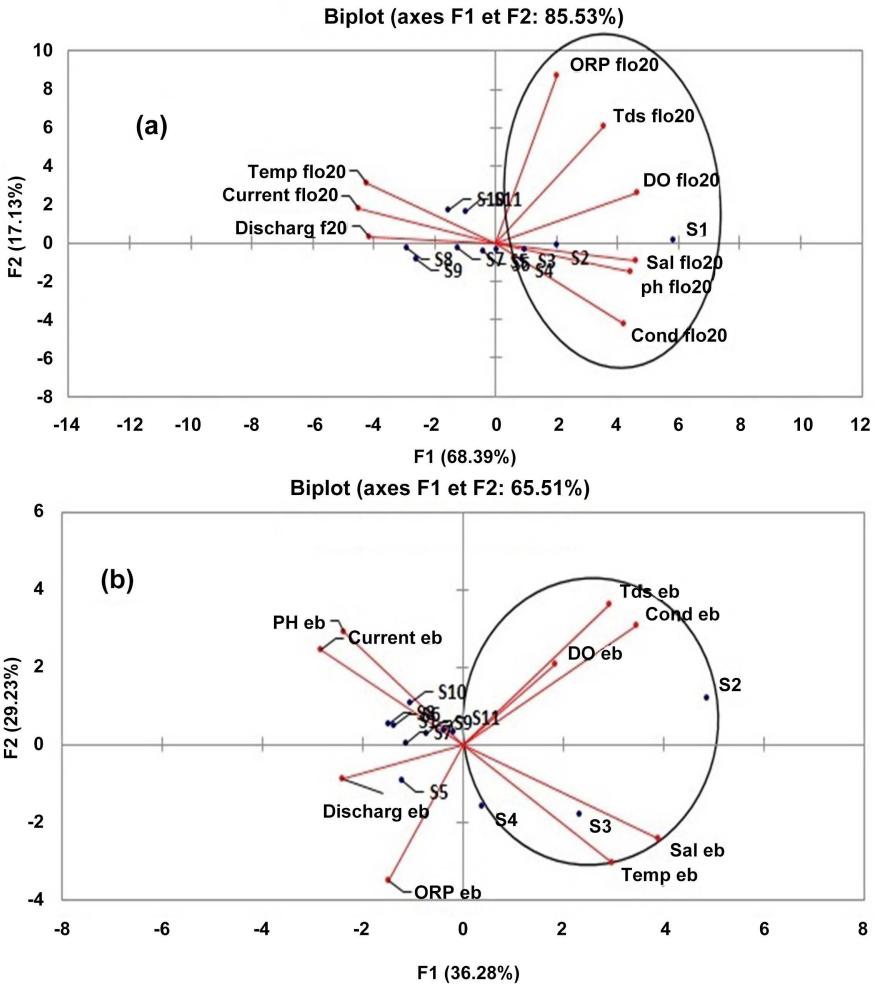

Figure 8. Lunar influence on the monitored water parameters. With (a) and (b) representing spring and neap tide respectively.

Seasonal dynamics: at seasonal scale, the low water regime of the dry period (Figure 7(c)) showed that, the stations S1, S2, S3, S4 and S5 were linked by ORP,

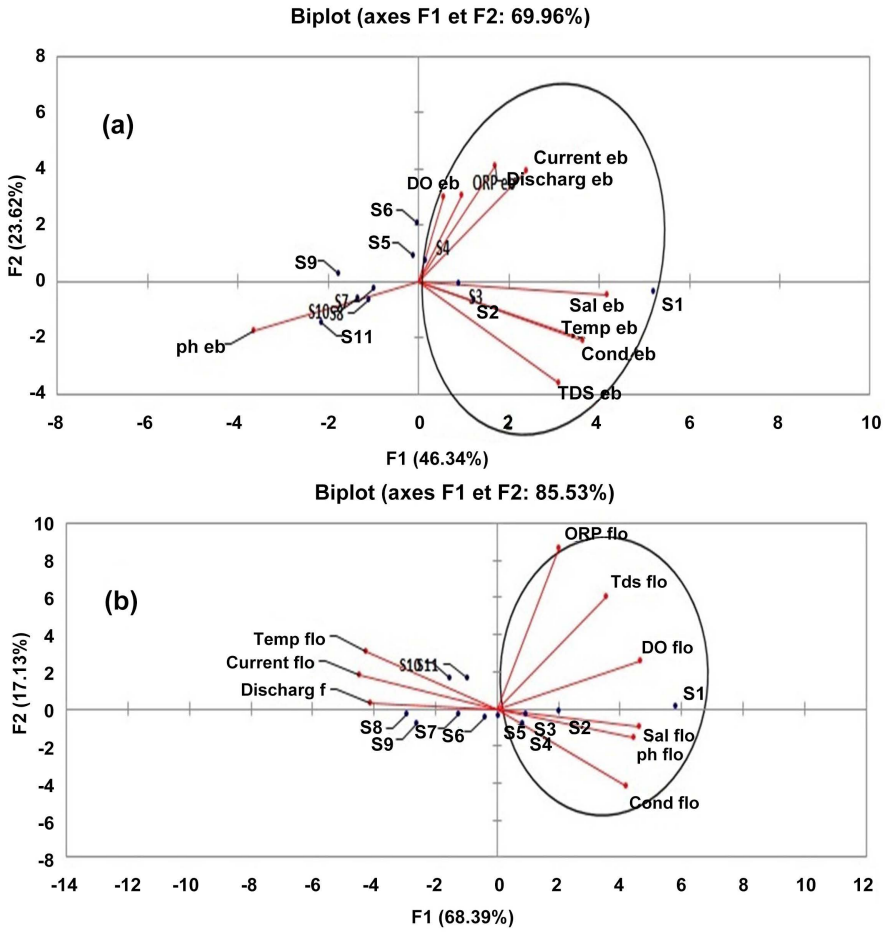

Figure 9. Diurnal effect with (a) and (b) representing ebb and flood tide respectively.

DO, Salinity, pH, conductivity and TDS. Except for temperature, surface current and discharge volumes, all the other variables were positively correlated with salinity at the F1 plan (40% contribution). Examples of the positive correlations presented by salinity were those with TDS (r = 0.66) and conductivity (r = 0.91). These correlations were poor (near to zero) around S5 (limit of Bonalokan, 8km from the Bridge). The average season revealed a different set of associations within these parameters (**Figure 7(b)**). Here, the F1 factorial plan (47% contribution) revealed that, S1, S2, S3 and S4 (intrusion limit of Bangue, about 4km from S1) were linked by Temperature, Salinity, DO, Conductivity and TDS. These variables also gave a negative relation with the hydrometric parameters (surface current and discharge). The most important correlation coefficient (r = 0.86) of salinity was found with both Temperature and DO. These correlation coefficients reduced with conductivity (r = 0.49) and TDS (r = 0.46). The average picture for wet period showed that, S1 and S2 (Bangue) were linked by TDS, salinity and temperature (**Figure 7(a)**). At this level salinity revealed a good correlation (r = 0.77) with temperature only. These positive correlations dropped to r = 0.39 and r = 0.34 with TDS and conductivity respectively. Surface current and discharge (hydrometric variables) have antagonistic effect on the water quality

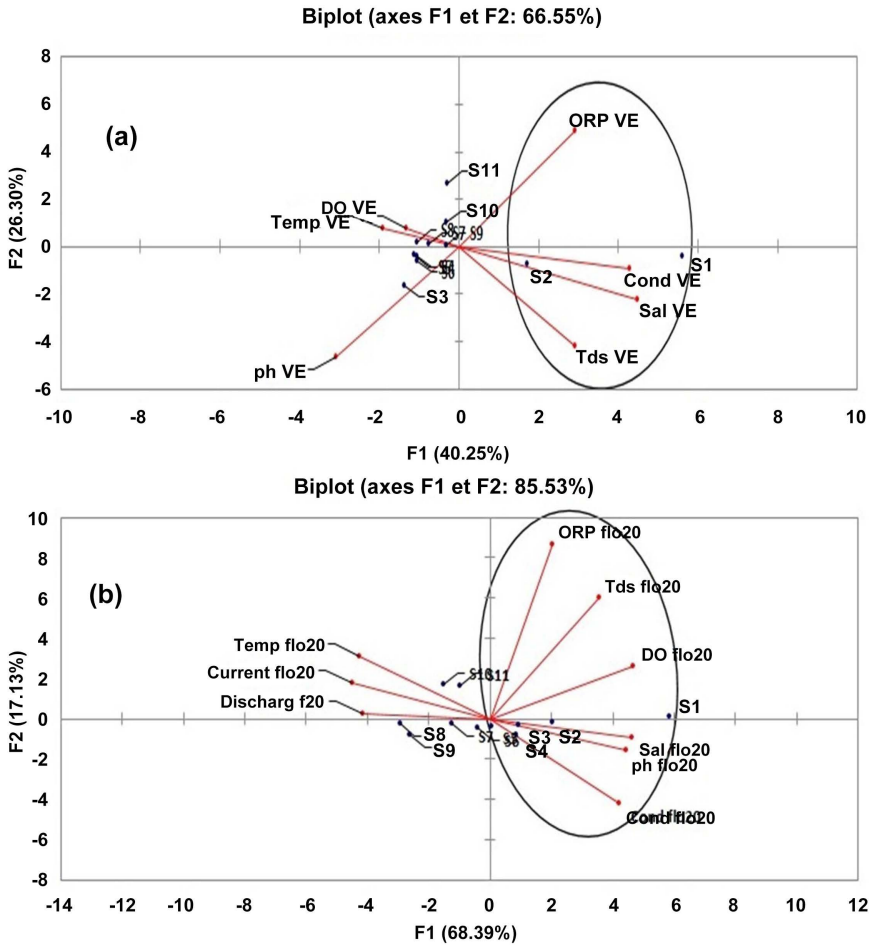

Figure 10. Inter-annual comparison of spring tide dynamics with (a) and (b) representing spring 2019 and spring 2020 conditions.

parameters; while surface current presented a low positive correlation, discharge volume revealed a negative association with salinity (Figure 7(a)).

Lunar variation: looking the lunar scale (Figure 8), the spring tide (Figure 8(a)) revealed that, salinity showed a strong affinity with DO, pH, Conductivity and TDS in the F1 factorial plan (68.39% contribution). The correlation coefficients obtained here were r = 0.86, 0.77, 0.85 and 0.60 for salinity and DO, pH, Conductivity and TDS respectively. The stations S1 to S5 were interconnected through the above parameters and S5 indicated the limit of salinity intrusion. At neap tide (Figure 8(b)), this frontier seems to be located in S4. At this time, salinity gives positive correlation with TDS, conductivity, DO and temperature (F1 plan with 36% of contribution). The strongest coefficients of salinity here is that with temperature (r = 0.77). This results also revealed that, the residual snapshot of both spring and neap tidal regimes showed surface current and discharge volume anti correlated with salinity and its associated water parameters (TDS, DO and Conductivity) (Figure 8(a) and Figure 8(b)).

Diurnal vibration: Figure 9 of the picture of the diurnal dynamic presented an ebb tide condition (Figure 9(a)) in which S1, S2 and S3 (intrusion frontier)

were associated by salinity, temperature, Conductivity, TDS, DO, ORP, Surface current and discharge volumes (in the F1 plan of 46% contribution). The positives correlations coefficients of salinity were r = 0.89, 0.78 and 0.73 recorded with conductivity, temperature and lastly TDS respectively. Discharge volumes, surface current, ORP and DO presented non-significant correlation coefficients (with salinity) of r = 0.34, 0.56, 0.15 and 0.02 respectively. During flood tide condition, (**Figure 9(b)**), the stations S1 to S5 (frontier point) were linked by salinity, pH, conductivity, DO, TDS and ORP in the F1 plan (68.39% of contribution). At this stage, salinity highlighted positive correlations with DO (r = 0.86), pH (r = 0.77) and conductivity (r = 0.84). Furthermore, surface currents and discharge volume highlighted an inverse effect on salinity and it related parameters during the flood condition.

Inter-annual evolution: the comparison between the spring tides of the year 2019 and that of 2020 (**Figure 10**) revealed two distinct spanning of the monitored water quality parameters. In 2019 (**Figure 10(a)**), salinity gave good correlations with TDS (r = 0.79) and Conductivity (r = 0.74). Its deployment also revealed that, the intrusion frontier was located at S4 (Bangue). On the order hand, the year 2020 presented a more extended (about 4km up stream) saline water frontier (Bonalokan or S5). This time, the association between these stations was built on their affinities with conductivity, pH, DO, TDS and ORP. The above parameters showed these linkages in the F1 factorial plan that have contributions of 40.25% and 68.39% for 2019 and 2020 respectively.

4. Discussions

4.1. Dynamics of Water Quality Parameters

The spatial variation of water temperature showed distincts temporal appearances at the seasonal, lunar and diurnal scales (**Figures 2-4**). The seaonal variation (**Figure 2**) is directly attributed to the climate of the study area, which is unsually characterized by a hot dry season and a cold wet period with heavy rainfall. The unexpected higher temperature registered during the wet season compared to the average water period snapshot could be explained by specific atmospheric forcing (cloud couverd, solar radiation and wind stress) [10] during the sampling periods and other prosses such as rain squall and anthropic processes. This situation is different from that obtained by [28] where precipitations freshens surface waters and reduce the temperature of surface water. The difference between these two results could be explained by the fact that, the present study took place in the upper estuarine environment while the previous took place in the open ocean with very little terrestial influence. The lunar scale (**Figure 3**) showed a tendency different from other tropical estuaries in which spring tides are colder than neap tides conditions. This difference could be explained by the fact that, the present study took place in th upper section of the Cameroon estuary that received waste water (warmer water) from domestic, industrial and the Douala harbor activities opposite to the lower section studied in

tropical estuaries, that receive fresher water from marine environments [29]. This upper section is also strongly influence by terrestial warming of it sorrounding. The poor domination of either flood or ebb tide at the diurnal scale (**Figure 4**) could be explained by the fact that, the daily temperature of water depends directly on the atmospheric forcing (solar radiation) that does not depend on the raising or falling of the water level. This also explained the temperature differences observed between the year 2019 (higher) and the year 2020 (lower values) (**Figure 5**). The spatial pathern in temperature between S1 to S11 (Bridge to Bona'Anja) is related to the fact that, temperature fluctuations depends on the geographical location (local features) of the catchement area, seasonal change, biological activities and impact of anthropogenic activities [30]. The length of the errobars revealed that, the water temperature do not change much during the wet season, neap phase and ebb conditions. This could be explained by the reduce influence of the water from the lower and the middle section of the estaury during these conditions.

Results from salinity analysis (**Figures 2-5**) exposed that, the upper section of the Cameroon estuary (Wouri-Nkam channel) is subjected to a spatial and temporal variability. The complete domination of the channel by freshwater during the average and wet seasons respectively (**Figure 2**) could be explained by the strong dilution from the intense precipitation occuring during these periods. Oppositely, the residual dry period, lunar phases and the diel tides conditions revealed two zones (oligohaline and limnic zones), this axial stractification could be explained by the tidal influence (tidal prisms) couple to the reduce rainfall with lower river runoff and stronger evaporations during these scales. The inter comparison of salinity distribution between tidal conditions with similar intensities during the years 2019 and 2020 reveal that, the spring tide of 2020 was more intense and extended traces of salinity up to S4 (0.3 psu) while it corresponding spring condition in 2019 was limited to S3 (s = 0.1 psu). This inter tidal dynamics between spring periods of 2019 and 2020 could be explain by the differences in atmospheric and hydrodynamics forcings (precipitation, evaporation, river runoff, wind, tidal pumping) [10] [31] [32] couple to the domestic and industrial (from the douala harbour) dumping between these two years. Oppositely the neap tide regime of 2019 (S1 = 3.4 psu) was more intense compare to that of 2020 (S1 = 0.1 psu). this unexpected domination of 2019 in neap periods images maybe resulting from percolation through dirty areas, infiltration of marine water into the ground water aquifers due to dredging, dumping of human waste (Urine), industrial extractons soda and potash [33] couple to differences in precipitation, evaporation, sand mining and mangroves stand destruction. The bathymetric point of view elucidated from dredging, sand mining, mangrove distruction of mangroves stands and land reclamation is explained by the fact that, deeper estuary can leads to a shift upstream of salinity intrusion and vice versa [34]. The length of the errorbars in **Figure 2(b)**, **Figure 3(b)** and **Figure 4(b)** showed that in terms of salinity, the dry period, spring phase and flood tide were

more dynamic (longest errorbars) compared to their corresponding wet period, neap and ebb tide. Similarly, the year 2020 (spring tide) was more dynamic compare to 2019. Again this strong dynamic conditions could be attributed to the greater marinisation that accompanied these situations.

TDS showed similar tendencies with salinity at seasonal, lunar and diurnal scales (**Figures 2-4**). These axials TDS gradients picturing salinities could confirmed the conservative character of this parameter in the section of the estuary. Furthermore, the strong correlation (with r varying from 0.6 - 0.8) between TDS and salinity observed here is different from that obatined by [7] in the Douro estuary. In this latter, TDS is potentially produce within the estuary rather than in its lower end (revealling a non conservative character). This confirms that, estuaries are specific in term of TDS dynamics. The high TDS values in the lower stations (S1 and S2) could be explained by: 1) the dredging operations and turbulent activities in the Douala harbor that causes fines particles and polluants traps at the bottom to be release at the surface; 2) the bidirectional flow, combined to its tidal distortion intensity. Indeed, the tidal distortion causes flood currents to be more intense compare to it ebb current. The resulting strong erosion of the bedfloor consiquently increases the TDS value; and 3) the decomposition of organic materials by microbial organisms, the direct or indirect dumping of industrial wastes (passive loading of amonia). This results also revealed that, the lower section of this channel, composed of S1 and S2 have dispersive character, more erosive with a lower fall speed of particles compare to the upstream with a undirectional flow. At seasonal scale, the high TDS values recorded during the dry period (**Figure 2**) could be explained by activities in the Douala harbor and the more intense bidirectional flow occuring during this period. All these processes where potentially more important during spring and flood tides conditions (**Figures 3-5**).

DO is a particular useful parameter and an excellent indicator of water [35]. The relatively highest DO values obtained during the dry period (**Figure 2**) could be due to; 1) the reduction in flow intensity causing poor draining of organic material into the estuary [33], 2) availability of light with maximum temperatures and consiquently more photosynthesis and 3) the introduction of new marine or estuarine phytoplankton community that releases oxygen in the aquatic medium [7] [36]. On the other hand, the lower DO values obtained during average and wet season snapshot could be due intense respiration of organic matter from river runoff couple to the reduced photosynthesis [37]. These organic matters could originate from the over loading of oragnic matters from agricultural sites during heavy rain. Also, the spring phase of tide was better oxygenated because of the its greater tidal prisms compared to neap tide conditions (**Figure 3**). This disctinction was not clear at diurnal scale because both flood and ebb tide took place within the same day. At inter-annual time scale, the low values of dissolved oxygen (DO less than 2 mg/l = hypoxia conditions) obtained during 2020 could be linked to land reclamation operations, sewage

dumping and dredging activities going on; this operation were accompanied by the destruction of aquatic plants including mangrove stands that produce oxygen by photosynthesis. Other processes such as the oxidation of exposed soil could also be pronounced; this oxydation required oxygen for the conversion of most unoxidized metals (from newly expose soil after dredging) such as iron to their oxydized stable form. The spatial variablity (**Figures 2-4**) did not revealed a clear drift since it's the horizontal evolution also considere the micro climatic conditions and ecological niches of the various sampling stations. The length of the errorbars do not showed a clear domination at diurnal scale since the concentration of this variable depends on processes ranging from physical to biological including the chemical and interactions between them [35].

During this study, ORP values were found to be higher during spring and flood tides compare to their neap and ebb phases (**Figure 3** and **Figure 4**). This could be eplained by the large flux of brackish water that enter the frontal area during these former periods. The positive ORP values (about +200 mV) obtained throughout the studied period translate the domination of nitrification (+100 to +350 mV), biological phosphorus removal (+25 to +250 mV) and cBOD degradation (+50 to +250 mV) with molecular oxygen processes [38]. At these scales, the high ORP values in S10 and S11 could be explain by the high agricultural activities around these points. The trends in spatial and temporal domination among these processes is not clear as they depends on a wide range of factors.

In this study, the averag (mean) water and the wet period (**Figure 2**) presented pH values lower than 6. This implies acidic environment and could be attributed to the increase input of humic materials from associated swamps creeks, dilution from ionic concentration by acidic rain and poor buffering capacity [39]. This result is in good agreement with those obtained by [40] who founded that, the pH of rainwater in such urbanized tropical city is arround 5.6, indicating a corrossive charater that could result from excessive dilution of carbon dioxide gas. At lunar scale, the acidic environment encounter during the neap phase of tide (**Figure 3**) could be attributed to the balance respiration-photosynthetic metabolisms couple to domestic and industrial disposal and the atmospheric partial pressure of carbon dioxide during the sampling periods. The above reason could be used to indicate the acidic character of the water during the year 2020 (**Figure 5**). Oppositely, the quasi neutrality of the water observed during the dry period (**Figure 2**), spring tide (**Figure 3**) and diel conditions (**Figure 4**) could be explained by the influence of tidal prism that bring in basic ocean water into the estaury during these periods. The errorbars revealed a more dynamic average water season, neap phase and ebb tides condition.

4.2. Dynamics of Surface Current and Discharge Volumes

Figure 6 showed that, the residual wet season has the highest surface currents (red line), followed by the mean/average water (green line) and lastly the dry pe-

riod (wet > meanwater > dry period). This situation is explained by the increase runoff from intense and continous precipitations occuring during the wet period. At spatial scale (horizontal evolution) the highest values of surface current and discharges volumes at S1 (Bridge) resulted from the geometric properties of the channel [41]. The surface currents reverse (negative/positives values) observed up to S6 and S7 (about 15km from the bridge) (**Figure 6**) during spring and flood conditions (red lines) respectively is as a result of the stronger tidal prisms that overcome the low river flow and pushes brackish water upstream reversing the river flow direction. However, simultanous high volume of fresh and brackish water in the Bridge (S1) could be explaine by the funnel effect in this segment [18] that causes a tidal amplification (tidal prism) or increases the ebb current and consiquently the volume discharge. Regarding the spatial scale, the surface current showed maximun values around the riverine end members (S7 to S11) at seasonal scale. This parthern in inverted at lunar and diurnal images as a result of the tidal contribution that may modifies the hydrodynamics circulation. Furthermore, the stronger currents uptream may be reduced by the mangrove strands near the bridge and Bonalokan (S4). The reduced river flow in the upstream direction may also highlight that, this estuary section follow an exponetial reduction in cross-sectional area and depth, hence it bathymetry.

4.3. Interactions and Dynamics of Salt Water Intrusion in the Upper Section of the Cameroon Estuary

In this section, we discussed the upstream intrusion of brackish from the PCA. The results obtained showed different spatial and temporal variations of salt or brackish water of the various sampling stations (S1 - S11). The frontier of salt water extended to S5 (8 km from the Bridge) during the residual dry season (**Figure 7(c)**), flood tides conditions (**Figure 9(b)**) and the spring phase (**Figure 8(a)**) of lunar scale. On the other hand, the high water (wet period), neap phase and ebb tides, have extension length limited S3 or S4 (4 km from the Bridge). At inter-annual level (**Figure 10**), the year 2020 has a more pronounce extension (up to S5) compare to the year 2019 (limited at S4). The vibrating distance of about 4 km observed within the temporal scale could be explained by changes in river discharge, atmospheric conditions, anthropic dumping of sewage couple to the tidal conditions. A prolonged analysis of this result revealed that, the position of the salinity intrusion limit varies inversely with river discharge and surface currents (**Figure 7(b)**, **Figure 7(c)**, **Figure 8** and **Figure 9**). These observations are similar to those obtained [18] [24] [32]. This could be explained by the fact, intense precipitations increase river runoff that in turn causes a tidal damping and hence tidal prism reduction in the lower segments. Inversely, low precipitation produces a river flow that is easily overcome by the tidal prism allowing the tidal prism to travel further upstream.

The temporal change in the hydrological signature within the frontal zone (**Figures 7-10**) could be related to changes in the hydrometric, biological, anthropogenic and atmospheric variable's intensities; the changes in the composition

of the various stations resulting from the numerous factors affecting estuaries dynamics exposed the complexity of the Wouri-Nkam section of the Cameroon estuary. In this case, change in land uses like land reclamation, dredging, tidal intensity, mangrove degradation and agricultural activities could enlighten the origin of the different factors changing the hydrodynamic parameters. The variation in water masses could have effects on the changing current intensities, discharge volumes, depth of the channel, biochemical processes, pollutants discharge and hence mixing of saline water that influence the water quality. These interactions could be important in the determination of the fishing structure and ecological status of this zone of this estuary.

4.4. Potential Impacts of the Tidal Intrusion (Frontier) Dynamics in the Wouri-Nkam Estuary

The analysis of variances (ANOVA) revealed that Temperature and DO varies significantly at inter-annual ($F = 0.73$, $df = 09$, $p < 0.05$) seasonal and lunar. In addition to these variables, significant variations were also obtained at lunar scale for Salinity, TDS and pH values ($df = 09$, $p < 0.05$). In this study, the dynamics of the salts intrusion zone highlighted an axial gradients of about 08 kilometers within the seasonal and lunar scales. This means that, the horizontal displacement of the Oligohaline water (Salinity ≥ 0.5 psu) could cause the fresh water species to reduce or increase their environment by 08 km. Since the salinity factor controls the fauna, flora and minerals distributions; for instance, saline water (30 - 35 psu) shelters stenohaline species (Branciopodes, crustaceans, and lamellibranches), Brackish water (1 - 30 psu) shelters some euryhaline and oligohaline species while fresh water (<0.5 psu) shelters fresh water organisms only. The salinity content and associated water quality obtained during the dry periods could explained the abondant clams observed by [42] in this section of the Cameroun estaury. Again, field observations of the fishes communities in this area, revealed a domination of the families of Arapaimidae, Ciclidae and Chanidae (by catche composition) during the dry period conditions. This study also reveal that, the ichthyoplankton abundance and the relative abundance of species (the Mockokidae, Claridae and Scilbeidae families) observed during the wet season (spawning season) could be due to the fact that, the water quality parameters were spatially more stable (not signficant at ($F = 0.48$, $df = 9$, $p < 0.05$) with a relatively low temperature (25.5˚C - 27˚C). However a fishe biometry is needed to understand the dynamics of fish composition associated to these tempral variations. The results of this study has enhance the understanding of the dynamics of the hydrological parameters necessary for the fisheries and fish farming activities (marine, brackish and fresh water species) practiced in this section of the estuary. Equally, the information in this work could be used not only to understand the ecology of endangered species of this estuary such as aquatic turtles, manatee and slams but also to explain the presence of diadromous species at distances greater than 20 km from the bridge during spring tide of the dry season.

The freshwater available for drinking and agricultural purposes for the local population before Yassem (S6) is therefore expose to salinization processes that may in turn impact their living conditions since they directly depends of the Wouri-Nkam river water for drinking, household needs, agricultural and fish farming purposes.

Temperature plays a crucial role in the distribution of living organisms in aquatic environment. The values of water temperature obtained in this study are similar to those registered in other tropical estauries [43]. These high tempertaures values (26˚C - 32˚C) could cause a change in the chemical and physical composition of water quality, density, viscosity reduction, solubility of important gas reduction, enhance evaporation and sedimentation [44]. Furthermore, since TDS is reletad to conductivity and salinity, it could be used to determined the upstream excursion of material (fine sediments and organic debris) from the middle section bearing the Douala harbor. This dedris and fine sediments could impact the water quality of the nursey grounds and the local fish ponds located before Bangue (S4).

The results of this investigation could be a tool for the indentifacation of potential hypoxia zones, since this hypoxia conditions could threats the life of many aquatic species [45], slow down the development of aquatic life and enhance biodiverty lost in the Wouri estuary. According to [45], coastal waters typically require a minimum of 4.0 mg/l but do better with 5.0 mg/l of oxygen to provide optimum ecosystem function and highest carrying capacity.

Finally, knowledge on the surface current is a good indicator of the sedimentation due to marine processes (salty sand availability are limited at 8 km from the Bridge). This work therefore revealed that pure fluvial sediments, suitable for housing constructions are located after S7 (Bonagando, 15 km from the Bridge) after a flood tide of the spring condition in the dry season.

5. Conclusion

The dynamics of the water quality parameters (Temperature, salinity, TDS, pH, surface current and discharge volumes) studied in the Cameroon estuary, central coast of Africa showed that, this area is characterized by a large range of temporal and spatial variations that are modulated by short terms tidal fluctuations and multi-scale seasonal evolutions cause by meteorological and/or weather forcings. The dynamics of the salts intrusion zone in the Wouri-Nkam estuary highlighted an axial gradient of about 08 kilometers at seasonal and lunar scales. The freshwater available for drinking and agricultural purposes for the local population before Yassem (S6) is therefore exposed to salinization processes that will in turn impact their living conditions since they directly depend on the Wouri-Nkam water for drinking, household needs, agricultural and fish farming purposes. The state of water quality (physico-chemical parameters) and the position of the saline water frontier have been determined but will require further monitoring together with other environmental stresses such as sea level rise,

land reclamation and occupation, geomorphological, demography and disposal from domestic or industrial dumping. This will further highlight the understanding of the functioning of this estuary since its dynamics is very complex and cannot be explained by physical processes alone. The knowledge of its biological, chemical and biochemical interactions should also be well understood in order to have a broad overview of its whole evolution. So, futures studies to buttress the results of this investigation should focus on:

- Time series sampling: the work focus on the spatial dynamics of the hydrological parameters during defined periods. The implication of long time series will permit to increase the investigation scale; from small scale hourly events to seasonal, including the influence of atmospheric forces, hence with a global view of the conditions influencing the dynamics of saline water intrusion frontier in this region.
- Assessment of environmental and anthropic activities: the environmental and anthropic activities influencing the hydrological parameters in this tidal intrusion zone should be well quantified and characterized.

Acknowledgements

This study is part of the *Wouri-Nkam ecosystems monitoring project* of the Centre of Tropical Aquaculture (CAT) of the Institute of Fisheries and Aquatic Sciences (ISH) of the University of Douala. The authors specially thank the Center of Tropical Aquaculture (CAT) for the housing facilities and the Institute of Fisheries and Aquatic Sciences (ISH) for the financial support. The authors also acknowledge colleagues and friends from the Department of Oceanography ISH: Dr. Oben Mbeng Lawrence, Dr. Abessolo Gregoire and Dr. Mama Crepin for their, advises and instrumental support during field measurements. Particular thanking goes to the students of the Department of Oceanography of ISH for their enthusiastic participation during field work. The field work of this study would not have been completed without the courage of the members of the Association for the Conservation of Nature (ASCON).

Conflicts of Interest

The authors declare no conflicts of interest regarding the publication of this paper.

References

[1] Sabater, S. and Stevenson, R.J. (2010) Foreword: Global Change and River Ecosystems—Implication for Structure, Function and Ecosystem Services. In: Stevenson, R.J. and Sabater, S., Eds., *Global Change and River Ecosystems—Implications for Structure*, *Function and Ecosystem Service*, Vol. 215. Springer, Dordrecht, 1-2. https://doi.org/10.1007/978-94-007-0608-8_1

[2] Fantong, W.Y., Kamtchueng, B.T., Ketchemen-Tandia, B., Kuitcha, D., Ndjama, J., Fouepe, T.A., Gloria, E., Takem Mengnjo, I., Wirmvem, J., Bopda Djomou, L.S., Ako, A.A., Nkeng, G.E., Kusakabe, M. and Ohba, T. (2016) Variation of Hydrogeo-

chemical Characteristics of Water in Surface Flows, Shallow Wells, and Boreholes in the Coastal City of Douala (Cameroon). *Hydrological Sciences Journal*, **61**, 2916-2929. https://doi.org/10.1080/02626667.2016.1173789

[3] Davies, O.A. and Ugwumba, O.A. (2013) Tidal Influence on Nutrients Status and Phytoplankton Population of Okpoka Creek, Upper Bonny Estuary, Nigeria. *Journal of Marine Biology*, **2013**, Article ID: 684739. https://doi.org/10.1155/2013/684739

[4] Freeman, L.A., Miller, A.J., Norris, R.D. and Smith, J.E. (2012) Classification of Remote Pacific Coral Reefs by Physical Oceanographic Environment. *Journal of Geophysical Research*: *Oceans*, **117**, Article No. C02007. https://doi.org/10.1029/2011JC007099

[5] Pierce, D.W., Gleckler, P.J., Barnett, T.P., Santer, B.D. and Durack, P.J. (2012) The Fingerprint of Human-Induced Changes in the Ocean's Salinity and Temperature Fields. *Geophysical Research Letters*, **39**, Article No. L21704. https://doi.org/10.1029/2012GL053389

[6] Dolgopolova, E.N. and Isupova, M.V. (2010) Classification of Estuaries by Hydrodynamic Processes. *Water Resources*, **37**, 268-284. https://doi.org/10.1134/S0097807810030024

[7] Azevedo, I.C., Duarte, P.M. and Bordalo, A.A. (2006) Pelagic Metabolism of the Douro Estuary (Portugal) Factors Controlling Primary Production. *Estuarine*, *Coastal and Shelf Science*, **69**, 133-146. https://doi.org/10.1016/j.ecss.2006.04.002

[8] Largier, J.L. (1992) Tidal Intrusion Fronts. *Estuaries*, **15**, 26-39. https://doi.org/10.2307/1352707

[9] Kimmerer, W. (2002) Effects of Freshwater Flow on Abundance of Estuarine Organisms: Physical Effects or Trophic Linkages? *Marine Ecology-Progress Series*, **243**, 39-55. https://doi.org/10.3354/meps243039

[10] Maes, C., Dewitte, B., Sudre, J., Garcon, V. and Varillon, D. (2013) Small-Scale Features of Temperature and Salinity Surface Fields in the Coral Sea. *Journal of Geophysical Research*: *Oceans*, **118**, 5426-5438. https://doi.org/10.1002/jgrc.20344

[11] Tyler, M.A., Coats, D.W. and Anderson, D.M. (1982) Encysament in a Dynamic Environment: Deposition of Dynoflagellate Cysts by a Frontal Convergence. *Marine Ecology Progress Series*, **7**, 163-178. https://doi.org/10.3354/meps007163

[12] Toole, J.M. and McDougall, T.J. (2001) Chap. 5.2 Mixing and Stirring in the Ocean Interior, in Ocean Circulation and Climate. *International Geophysics*, **77**, 337-355. https://doi.org/10.1016/S0074-6142(01)80127-3

[13] Ridgway, K.R. and Dunn, J.R. (2003) Mesoscale Structure of the Mean East Australian Current System and Relationship with Topography. *Progress in Oceanography*, **56**, 189-222. https://doi.org/10.1016/S0079-6611(03)00004-1

[14] Jewell, P.W., Stallard, R.F. and Mellor, G.L. (1993) Numerical Studies of Bottom Shear Stress and Sediment Distribution on the Amazon Continental Shelf. *Journal of Sedimentary Petrology*, **63**, 734-745. https://doi.org/10.1306/D4267C7B-2B26-11D7-8648000102C1865D

[15] Nikiema, O., Devenon, J. and Baklouti, M. (2007) Numerical Modelling of the Amazon River Plume. *Continental Shelf Research*, **27**, 873-899. https://doi.org/10.1016/j.csr.2006.12.004

[16] Fontes, R.F.C., Castro, B.M. and Beardsley, R.C. (2008) Numerical Study of Circulation on the Inner Amazon Shelf. *Ocean Dynamics*, **58**, Article No. 187. https://doi.org/10.1007/s10236-008-0139-4

[17] Olivry, J.C. (1974) Regime hydrologique du fleuve Wouri et estimation des apports recus par l'estuaire et la mangrove du Wouri. Office de la recherche scientifique et technique outre-mer, ORSTOM. Republique unie du Cameroun, 60 p.

[18] Onguene, R., Pemha, E., Lyard, F., Du-Penhoat, Y., Nkoue, G., Duhaut, T., Njeugna, E., Marsaleix, P., Mbiake, R., Jombe, S. and Allain, D. (2015) Overview of Tide Characteristics in the Cameroon Coastal Areas Using Recent Oberservations. *Open Journal of Marine Sciences*, **5**, 81-98. https://doi.org/10.4236/ojms.2015.51008

[19] Ndongo, B., Lako, M.S., Awe Tirmou, A.A., Ntankouo, N.R. and Moukouri Dalle, J.D. (2015) Tendances pluviometriques et impact de la maree sur le trainage en zone d'estuaire: Cas du wouri au Cameroun. *Afrique Science*, **11**, 173-183.

[20] Fotsi Fossi, Y., Brenon, I., Pouvreau, N., Onguene, O., Yann, F., Njombe, D., Thibault, C. and Etame, J. (2020) Dynamique du maximu de turbidité dans le système estuarien du Wouri (Cameroun). *XVI*^{emes} *Journées national du Génie Cotier-Genie Civil*, Le Havre, 8-10 December 2020, 221-232. https://doi.org/10.5150/jngcgc.2020.025

[21] Mbusnum, K.G., Malleret, L., Deschamps, P, Khabouchi, I., Asia, L., Lebarillier, S., *et al.* (2020) Persistent Organic Pollutants in Sediments of the Wouri Estuary Mangrove, Cameroon: Levels, Patterns and Ecotoxicological Significance. *Marine Pollution Bulletin*, **160**, Article ID: 111542. https://doi.org/10.1016/j.marpolbul.2020.111542

[22] Olinga, O.J.M. (2011) Vulnerability of Urban Spaces and Local Strategies for Sustainable Development. Case Study of the City of Douala. Research Laboratory, Planning and Sustainable Development, University of Derby, Derby, 161 p.

[23] Willy, S.E. (2016) Analyse de la vulnérabilité du littoral du Wouri: Cartographie des zones à risques d'inondation à Douala. Mémoire d'ingénieur Halieute de l'Institut des sciences halieutiques de l'université de Douala.

[24] Koutitonsky, V. (2005) Oceanographic Sensors for the Environmental Monitoring System of the Douala Autonomous Harbour. Technical Report, Hydrosorft, S.A., Saint-Zotique.

[25] Allen, G.P., Salomon, J.C., Bassoullet, P., Du Penhoat, Y. and De Grandpre, C. (1980) Effects of Tides on Mixing and Suspended Sediments Transport in Microtidal Estuaries. *Sedimentary Geology*, **26**, 69-90. https://doi.org/10.1016/0037-0738(80)90006-8

[26] Bennasser, L. (1997). Diagnose de l'état de l'environnement dans la plaine du Gharb: suivi de la macro-pollution et ses incidences sur la qualité hydrochimique et biologique du bas Sebou. Thèse de doctorat d'état es science. Université Ibn Tofail, Kénitra, Maroc, 157 p.

[27] El Morhit, M., Fekhaoui, M., Serghini, A., El Blidi, S., El Abidi, A., Bennaakam, R., Yahyaoui, A. and Jbilou, M. (2008) Impact de l'aménagement hydraulique sur la qualité des eaux et des sédiments de l'estuaire du Loukkos (côte atlantique, Maroc). *Bulletin de l' Institut Scientifique*, *Rabat*, *section sciences de la terre*, No. 30, 39-47.

[28] Boutin, J., Martin, N., Reverdin G., Yin, X. and Gaillard, F. (2013) Sea Surface Freshening Inferred from SMOS and ARGO Salinity: Impact of Rain. *Ocean Science*, **9**, 183-192. https://doi.org/10.5194/os-9-183-2013

[29] Rossi, N. (2008) Ecologie des communautés planctoniques méditerranéennes et étude des métaux lourds (Cuivre, Plomb, Cadmium) dans déférents compartiments de deux écosystèmes côtiers (Toulon, France). These de doctorat de L'université du Sud Toulon-Var.

[30] DWAF (Department of Water Affaires and Forestry) (1996) South Africans Water

Guidelines. Vol. 7, Department of Water Affaires and Forestry, Pretoria.

[31] Matthews, A.J., Baranowski, D.B., Heywood, K.J., Flatau, P.J. and Schmidtko, S. (2014) The Surface Diurnal Warm Layer in the Indian Ocean during CINDY/DYNAMO. *Journal of Climate*, **27**, 9101-9122. https://doi.org/10.1175/JCLI-D-14-00222.1

[32] Hoagland, P., Beet, A., Ralston, D., Parsons, G., Shirazi, Y. and Car, E. (2020) Salinity Intrusion in a Modified River-Estuary System: An Integrated Modeling Framework for Source-to-Sea Management. *Frontiers in Marine Science*, **7**, Article No. 425. https://doi.org/10.3389/fmars.2020.00425

[33] El Morhit, M. and Latifa, M. (2014) Study of Physico-Chimical Parameters of Water in the Loukkos River Estuary (Larache, Morocco). *Environmental Systems Research*, **3**, Article No. 17. https://doi.org/10.1186/s40068-014-0017-7

[34] MacCready, P. and Geyer, W.R. (2010) Advances in Estuarine Physics. *Annual Review of Marine Science*, **2**, 35-58. https://doi.org/10.1146/annurev-marine-120308-081015

[35] Lajaunie-Salla, K. (2016) Modélisation de la dynamique de l'oxygène dissous dans l'estuaire de la Gironde. Sciences de la Terre. Thèse de doctorat phD, Université de Bordeaux, Bordeaux.

[36] Alpine, A.E. and Cloern, J.E. (1992) Trophic Interactions and Direct Physical Effects Control Phytoplankton Biomass and Production in an Estuary. *Limnology and Oceanography*, **37**, 946-955. https://doi.org/10.4319/lo.1992.37.5.0946

[37] Chicharo, M.A., Chicharo, L. and Morais, P. (2006) Inter-Annual Differences of Ichthyofauna Structure of the Guadiana Estuary and Adjacent Coastal Area (SE Portugal/SW Spain): Before and after Alqueva Dam Construction. *Estuarine, Coastal and Shelf Science*, **70**, 39-51. https://doi.org/10.1016/j.ecss.2006.05.036

[38] Gerardi, M.H. (2007) ORP Management in Waste Water as an Indicator of Processes Efficiency. YSI Environmental Application Note. New England Interstate Water Pollution Control Commission (NEIWPCC), Newsletter Interstate Water Reports. YSI Inc., Yellow Springs.

[39] Akpan, E.R., Offem, J.O. and Nya, A.E. (2002) Baseline Ecological Studies of the Great Kwa River, Nigeria 1: Physic Chemical Studies. *Africans Journal of Environmental Pollution and Health*, **1**, 83-90.

[40] Udoessien, E.I. (2003) Basic Principles of Environmental Sciences. Etiliew International Publishers, Uyo Nigeria, 339 p.

[41] Hume, T.M. and Bell, G.R. (1993) Methods for Determining Tidal Flow and Material Fluxes in Estuaries Cross-Sections. Water Quality Centre Publication No. 22, Water Quality Centre, Hamilton.

[42] Bang, G.E., Nwuith, A.G., BitjaNyom, A.R., Besack, F., Essome, C.M.M., La Fortune Fouegap, B. and Eyango, M.T.-T. (2020) Study of the Composition and Determination of the Micro-Algal Content in the Stomach of Clams (Bivalvia: Veneridae) of the Nkam-Wouri River Basin in Cameroon. *International Journal of Fauna and Biological Studies*, **7**, 105-113.

[43] Gillet, P. (1986) Contribution à l'étude écologique des Annélides Polychètes de l'estuaire du Bou Regreg (Maroc). Thèse de 3 ème cycle, Université d'Aix-Marseille (France), 215 p.

[44] Rabalais, N.N., Levin, L.A., Turner, R.E., Gilbert, D. and Zhang, J. (2010) Dynamics and Distribution of Natural and Human-Caused Coastal Hypoxia. *Biogeosciences*, **7**, 585-619. https://doi.org/10.5194/bg-7-585-2010

[45] United Nation for Education Scientific and Cultural Organization and the world

health Organization (1978) Water Quality Survey. Reports in Hydrology, No. 23, United Nation for Education Scientific and Cultural Organization and the world health Organization, Paris.